LEGIBILITY NOTICE

A major purpose of the Technical Information Center is to provide the broadest dissemination possible of information contained in DOE's Research and Development Reports to business, industry, the academic community, and federal, state and local governments.

Although a small portion of this report is not reproducible, it is being made available to expedite the availability of information on the research discussed herein.

LA-UR -87-2679

CONF-8708110--8

Los Alamos National Laboratory is operated by the University of California for the United States Department of Energy under contract W.-7405-ENG-36

LA-UR--87-2679

DE87 014732

TITLE THIN FILM MICROSTRUCTURES: SIMULATION AND THEORY

AUTHOR(S): A. Mazor
D. J. Srolovitz
P. S. Hagan
B. G. Bukiet

SUBMITTED TO The SPIE's 31st Annual International Technical Symposium on Optical and Optoelectronic Applied Science and Engineering, held August 16-21, 1987, San Diego, Ca.

DISCLAIMER

Los Alamos Los Alamos National Laboratory
Los Alamos, New Mexico 87545

Thin Film Microstructures: Simulation and Theory

A. Mazor, D. J. Srolovitz, P. S. Hagan, and B. G. Bukiet

Los Alamos National Laboratory
Los Alamos, NM 87545

ABSTRACT

The nature of the microstructure of physical vapor-deposited films depends sensitively on the substrate temperature during deposition. At low temperatures the microstructure is porous and ballistic aggregation-like, at intermediate temperatures the microstructure is columnar, and at elevated temperatures the grains are three dimensional. These different microstructural regimes are known as Zone I, II, and III, respectively. A theoretical analysis is presented in which the temporal evolution of the columnar microstructure (Zone II) is studied. The columnar microstructure is shown to be a balance between shadowing (which results in Zone I microstructures) and surface diffusion (which tends to smooth the surface). In addition to predicting the proper microstructure, this analysis properly predicts the temperature at which the Zone II to Zone I microstructural transition occurs. Since bulk diffusion is negligible and surface diffusion controls the microstructure in Zone II, the microstructure in the bulk of the film, may be viewed as frozen and all microstructural evolution occurs at the current, or active, surface. A Monte Carlo computer simulation technique which models the microstructural evolution of the surface is presented. The simulation follows the temporal evolution of realistic three dimensional Zone II microstructures and accounts for growth competition between adjacent grains and the formation of film texture.

1. INTRODUCTION

The microstructure of physical vapor-deposited (PVD) films is known to be sensitive to deposition conditions, among which the substrate temperature T is of particular importance. Three different types of microstructures have been identified for vapor deposited films corresponding to three different substrate temperature regimes.[1,2] Zone I ($0 < T < T_1$, where $T_1 \sim 0.3\,T_m$ for metals, $\sim 0.24\,T_m$ for oxides, and T_m is the melting point of the film) is characterized by a porous structure of crystallites separated by voided regions, the thickness of which is of order a few hundred angstroms. In Zone II ($T_1 < T < T_2$, where $T_2 \sim 0.45T_m$) the film is made up of columnar-grains, separated by metallurgical grain boundaries (i.e. no porosity, widths of order 5-10 Å). In Zone III ($T > T_2$) the structure consists of equiaxed grains. However, the microstructural features in this zone are sensitive to the type of material.[3]

The nature of the surfaces of these films is correlated with the underlying microstructure.[4] In Zone I, the crystallites tend to have domed tops with rough surfaces. Zone II grains have smooth matt surfaces. Finally, in Zone III the surfaces are referred to as "bright", based on optical microscopy.

A number of suggestions have been made regarding the mechanisms underlying these three microstructural zones. Ballistic aggregation studies[5] have predicted the porous microstructure of Zone I, under the assumption of negligible diffusion at the lowest deposition temperatures. These studies compare favorably with the transmission electron microscopy observations.[3] The transition to Zone II with increasing temperature is generally viewed as due to increasing surface diffusivity. This view is supported by the Arrhenius grain size/temperature relation (at fixed film thickness) which yields the same activation energy as for surface diffusion.[6] Additional support is provided by the simulations of Müller.[7] Based on activation energy determinations, the transition to Zone III has been attributed to the importance of bulk diffusion at $T > 0.5\,T_m$. However, recrystallization and/or grain growth have also been suggested as possible candidates, responsible for this transition.

In the present paper, we present analytical and simulation results relating primarily to Zone II microstructures. First, we propose a nonlinear partial differential equation for the space-time evolution of the microstructure. This equation yields the onset temperature of Zone II (i.e. $T \sim 0.2T_m$), the band of unstable modes, and the steady-state columnar microstructures characterized by small amplitude, regular surface relief. This matt surface becomes smoother with increasing temperature. At $T \sim 0.5\,T_m$, the surface is smooth over um length scales. In order to provide a more concrete picture of the microstructure and its development in the surface diffusion controlled, Zone II regime, we present Monte Carlo computer simulation results of Zone II microstructural evolution. The microstructures, shown both parallel to and perpendicular to the growing surface, are in excellent correspondence with experimentally observed Zone II microstructures. The simulations explicitly consider both grain boundary energy and surface energy driven microstructural evolution.

II. THE SURFACE EVOLUTION EQUATION

We now propose a nonlinear one-dimensional partial differential equation describing the evolution of an arbitrary initial surface profile, $h(x, t = 0)$ under the joint influence of a constant uniform deposition rate J of

finite-size atoms (of radius δ), and surface diffusion.[8] The coordinate system employed is indicated in Fig. 1. In the continuum limit ($\delta \to 0$) the surface height grows uniformly with a rate J. When the impinging atoms are of finite size ($\delta \neq 0$), the local growth rate of the surface depends on the surface curvature. Following the suggestion of Leamy et al.,[9] we note that the center of an atom sitting on a surface is actually at a height δ above the surface. This implies that the deposition does not take place on the actual surface h(x,t), but on an imaginary surface displaced by δ from h(x,t). Depending on the surface curvature, K, the projected length of an element of this imaginary surface on the x-axis is either greater or smaller than the projected length of the corresponding element of h(x,t) (see Fig. 1). This implies that an element of the surface (h(x,t)) receives a net flux of atoms either greater (for $K > 0$) or smaller (for $K < 0$) than J. A simple geometric construction yields to leading order in δ:

$$h_t = J + \delta J K = J - \delta J \frac{h_{xx}}{(1+h_x^2)^{3/2}} \qquad (1)$$

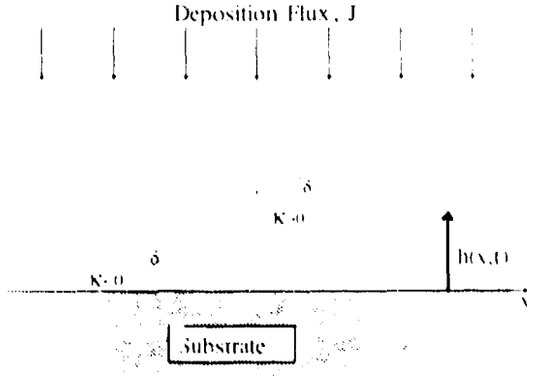

Figure 1. The film geometry (K is the surface curvature).

As mentioned above, surface diffusion plays a major role in the evolution of Zone II microstructures. Following Mullins,[10] we derive an expression describing the evolution of an arbitrary surface due to surface diffusion. Since the chemical potential μ of an atom on a curved surface is raised by $\sigma\Omega K$ (σ is the surface energy and Ω is the atomic volume) over that of a flat profile, the velocity of atoms along the surface v_s is

$$v_s = -\frac{D_s}{K_B T}\frac{\partial \mu}{\partial S} = -\frac{D_s \sigma \Omega}{K_B T}\frac{\partial K}{\partial S},$$

where D_s is the surface diffusivity, $K_B T$ is the thermal energy and S is an element of arc along the surface. The surface current of atoms is given by $r\,v_s$ where r is the number of atoms per unit area. Finally, the velocity of the surface normal to itself is

$$v_t = -\Omega \nabla_S (r v_s) = -D_e \nabla_S^4 K, \qquad (2)$$

where $D_e = D_s \sigma \Omega^2 r / K_B T$. In Cartesian coordinates, Eq. (2) may be written as

$$h_t = -D_e \left\{ (1+h_x^2)^{-1/2} \left| h_{xx}/(1+h_x^2)^{3/2} \right|_x \right\}_x \qquad (3)$$

The final equation describing the evolution of the surface under the combined action of surface diffusion and a constant deposition rate of finite size atoms is given by:

$$h_t = J - \delta J \frac{h_{xx}}{(1+h_x^2)^{3/2}} - D_e \left\{ \left(1+h_x^2\right)^{-1/2} \left| h_{xx}/\left(1+h_x^2\right)^{3/2} \right|_x \right\}_x \qquad (4)$$

Equation 4 may be written in dimensionless form by making the following change of variables:

$$H = \left(\frac{\delta J}{2D_e}\right)^{1/2}(h - Jt), \quad z = \left(\frac{\delta J}{2D_e}\right)^{1/2} x, \quad \text{and} \quad \tau = \frac{\delta^2 J^2}{4D_e} t.$$

This yields

$$H_\tau = -2\left(\frac{H_z}{(1+H_z^2)^{1/2}}\right)_z - \left\{ \left(1+H_z^2\right)^{-1/2} \left| \frac{H_z}{(1+H_z^2)^{1/2}} \right|_{zz} \right\}_z \qquad (5)$$

or by writing $g = H_z/(1+H_z^2)^{1/2}$

$$g_\tau = (1-g^2)^{3/2}\left\{ -2g_z - [(1-g^2)^{1/2} g_{zz}]_z \right\}_z. \qquad (6)$$

III. SURFACE EVOLUTION RESULTS

A. Linearized Results

The linearized version of Eq. (4) is sufficient to predict the transition between Zones I and II. In the small slope limit Eq. 4 reduces to

$$h_t = J - \delta J h_{xx} - D_e h_{xxxx}. \qquad (7)$$

Fourier decomposition of this equation yields

$$h(k,t) = Jt + h_0 e^{(\delta J k^2 - D_e k^4)t}, \qquad (8)$$

for a perturbation of a wavenumber k (or wavelength $\lambda = 2\pi/k$). The unstable (stable) modes are associated with positive (negative) arguments of the exponential in Eq. (8) (see Fig. 2). A band of unstable modes exist between $\lambda = \lambda_0 = (4\pi^2 D_e/\delta J)^{1/2}$ and $\lambda = \infty$, for an unbounded system. The maximally unstable mode has a wavelength: $\lambda_m = (8\pi^2 D_e/\delta J)^{1/2}$. These results imply that perturbations of wavelengths smaller than the diffusion length are smoothed by the surface diffusion, whereas the long wavelength perturbations grow unstably. The nonlinear terms, however, saturate the long wavelength instability into a relatively small amplitude columnar surface profile (see below)

Although Eq. (4) is a continuum equation the film itself is composed of discrete atoms. This implies that length scales smaller than a few δ are meaningless. As a consequence, when the diffusivity is so small that the diffusion length, $\lambda_0(T)$, is smaller than a few δ, it is as if D_e were identically zero in Eq. 4. Without this diffusion term to stabilize short wavelengths, the surface profile is unstable

with respect to perturbations of effectively any wavelength. Furthermore, the remaining nonlinear terms in Eq. 4 do not saturate any of these perturbations.

$2k^2-k^4$

$k_m \quad k_c \quad k$

Figure 2. The dimensionless dispersion relation for the perturbation modes of wavenumbers k. k_0 and k_m are associated with the shortest wavelength and maximally unstable modes, respectively.

Equating $\lambda_0(T)$ with few δ (we arbitrarily use 5δ), i.e., $5\delta = [4\pi^2 D_s(T)/\delta J]^{1/2}$, will yield a critical temperature, T_c, above which surface diffusion plays essentially any role in the microstructural evolution. Since D_s is proportional to D_s, which depends exponentially on temperature[7] ($D_s = D_0 e^{-Q/K_B T}$ where $Q = [5 + 20T/3T_m]K_B T_m$), T_c is relatively insensitive to variations around the minimum diffusion length ($\sim 5\delta$). Choosing $\sigma = 10^3$ dyne/cm, $\Omega = 2 \times 10^{-23}$ cm, $\delta = 4 \times 10^{-8}$ cm, and $J = 10^{-6}$ cm/sec, the equality $5\delta = \lambda_0(T)$ is satisfied at $T = T_c \simeq 0.2\,T_m$. This temperature is very close to the transition temperature T_1 between Zone I and Zone II ($T_1 = 0.24\,T_m$ for oxides and $0.3\,T_m$ for metals). We therefore conclude that the change in microstructure occurring at $T_1 = T_c$ is associated with the onset of effective surface diffusion.

B. Solution of the Nonlinear Growth Equation

While the linear analysis presented above is capable of predicting T_1, it is incapable of describing the experimentally observed columnar grain structure of Zone II. The microstructure is determined by the surface profile which is saturated by the nonlinear terms in Eq. 4. Employing a mathematical technique known as the "free energy" formalism we find that Eq. 4 reaches a steady state described by

$$H^2 = (1 + H_x^2)^{1/2} A \qquad (9)$$

where $-1 < A < \infty$ is an integration constant. This differential equation is solved by

$$x = \begin{cases} \dfrac{2A}{\sqrt{A+1}} F(\alpha, r) - 2\sqrt{A+1}\,E(\alpha, r) & A > -1,\ -\dfrac{\pi}{2} < \theta < \dfrac{\pi}{2} \\ \sqrt{2}\,[F(\beta, 1/r) - 2E(\beta, 1/r)] & 0 < |A| < 1,\ -\arcsin A < \theta < \dfrac{\pi}{2} \end{cases} \qquad (10)$$

where

$$\alpha = \arcsin\left|\left(\frac{1-\sin\theta}{2}\right)^{1/2}\right|,$$

$$\beta = \arcsin\left|\left(\frac{1-\sin\theta}{1+A}\right)^{1/2}\right|,$$

$$r = \left(\frac{2}{A+1}\right)^{1/2}, \text{ and } \theta = \arcsin(h^2 - A).$$

F and E are incomplete elliptical integrals of the first and second kinds, respectively.

The steady state profiles, corresponding to Eqs. (9-10) are indicated in Fig. 3 for several choices of the undetermined constant, A. These profiles are all oscillatory and periodic with a wavelength which decreases monotonically with increasing A. For $A > 0$, these profiles may be described as circular regions connected by lines of infinite slope. Such profiles correspond to simple solutions of Eq. 6, i.e. a sawtooth in g(x) between g = 1 and -1. In order to demonstrate that these solutions are stable steady states, we numerically solve the full nonlinear, partial differential growth equation (Eq. 6) for sinusoidal (Fig. 4) and random (Fig. 5) initial conditions using an implicit, finite-difference Crank-Nicolson scheme.[8] These numerical results clearly show that the predicted steady state solutions (Eqs. 9 and 10) are stable. However, Fig. 5 shows that once infinite slope regions are formed there is little additional evolution of the profile and hence the oscillations can be irregular with no well defined wavelength. When the initial deviations from a flat substrate are small, the wavelength of the surface profile will be determined by the maximally unstable mode of the linearized equation (i.e. λ_m, see Section III.A). This wavelength varies from approximately 10^{-5} cm at $T = 0.3\,T_m$ to 10^{-4} cm at $T = 0.5\,T_m$ and is of order the wavelength of light. This roughness in the surface profile may be the cause of the matted surface finish in Zone II.

$A = 10$

$A = 2$

$A = 0$

$A = 0.5$

Figure 3. The steady-state analytic solutions of Eq. 4, for various values of the undetermined constant of integration A.

It is of interest to note that the oscillatory surface profile which consists of circular caps is stable because the gradient in curvature along the surface is everywhere zero and hence there is no surface diffusion. In real materials, where the surface energy is not isotropic, the morphology of the steady state (no surface diffusion) film surface is not generally circular and may be determined by use of a Wulff plot. For a large number of materials, the surface energy anisotropy is such that the film surface will show faceted oscillations. Such crystallographically faceted surfaces are common morphological surface features in vapor deposited films.

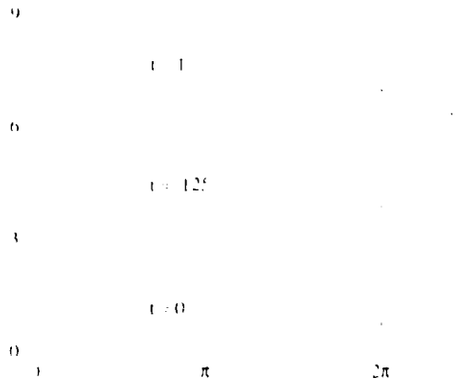

Figure 4. The steady-state numerical solution of Eq. 4, for a sinusoidal initial condition, as obtained at t = 1. Also shown are transient profiles.

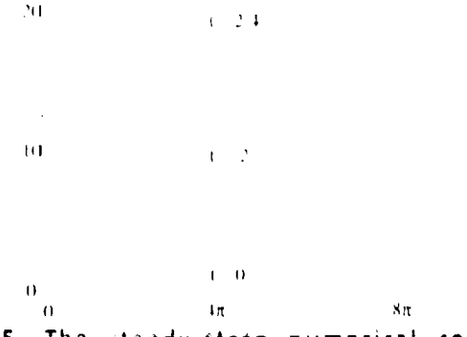

Figure 5. The steady-state numerical solution of Eq. 4, for a random initial condition, as obtained at t = 2.4. Also shown are transient profiles.

C. Grain Boundary Effects

The surface profile is modified by the presence of grain boundaries intersecting the growing surface. At the point of intersection, a groove with an opening angle ϕ is formed (see Fig. 6). This groove opening angle is determined by Young's equation to be

$$\phi = 2\cos^{-1}\left(\frac{\sigma_{gb}}{2\sigma_s}\right) \qquad (11)$$

where σ_{gb} and σ_s are the grain boundary and surface energy densities, respectively. For grain sizes, d, smaller than λ_m Eq. (11) is satisfied by a smooth, circular surface between grain boundaries (see Fig. 6a). On the other hand, for $d > \lambda_m$ diffusion is incapable of smoothing the surface over length scales comparable to the grain size and the rough surface morphology is obtained (Fig. 6b).

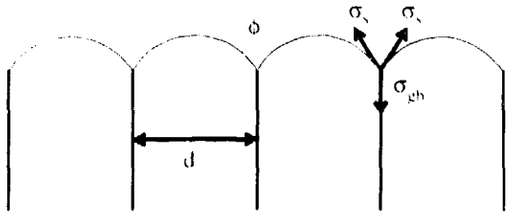

Figure 6a. Smooth circular surface between grain boundaries, for $d < \lambda_m$, where d is the grain-size, and λ_m is the wavelength of the maximally unstable mode. σ_s and σ_{gb} are the surface and grain-boundary energy densities, respectively. ϕ is the opening angle of the groove.

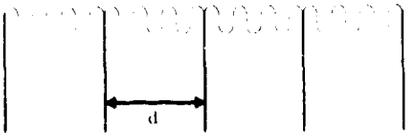

Figure 6b. The rough surface morphology obtained for $d > \lambda_m$ (see text).

For $d < \lambda_m$ (Fig. 6a), the total energy of the system is reduced by coarsening of the grain size. This coarsening process, as discussed above, only occurs by translation of the intersection of the grain boundary with the growing surface. If all of the circular grain caps do not have the same curvature, a net flux of atoms will occur across the grain boundaries such that the velocity of the grain boundary surface interaction parallel to the surface, v, is given by

$$v = a\nabla K , \qquad (12)$$

where a is a constant. This implies that the mean grain size, $\langle d \rangle$, will grow as

$$\langle d \rangle^3 = at + \beta$$

$$\langle d \rangle \approx a' t^{1/3} \qquad (13)$$

where a' and β are constants and the second relation is valid in the limit that $\langle d \rangle^3 \gg \beta$ (i.e. late times). A $t^{1/3}$ growth law is typical of diffusion limited growth process. $\langle d \rangle$ is of order λ_m the surface morphology changes from circularly capped grains to the oscillatory profile indicated in Fig. 6b. Since the spacing of the surface oscillations does not vary, once formed, $\langle d \rangle$ eventually becomes fixed at $\langle d \rangle \approx \lambda_m$. Therefore, a film viewed in cross section will have grains which on average, will increase in size with the distance from the substrate and saturate at $\langle d \rangle \approx \lambda_m$.

In this grain growth analysis we limited ourselves to two spatial dimensions (i.e. a one dimensional surface), where grain boundaries are lines. In a real film, grain boundaries are interfaces that generally have curvatures of order $1/\langle d \rangle$. Ignoring the surface curvature for the moment, the curvature of the grain boundaries themselves drives the motion of grain boundaries at their points of intersection with the surface. For this type of growth we find the mean grain size $\langle d \rangle$ to evolve in time as:

$$\langle d \rangle_t = a'' K = a''/\langle d \rangle \tag{14a}$$

$$\langle d \rangle = a''' t^{1/2}, \tag{14b}$$

where a'' and a''' are constants. This $t^{1/2}$ grain size dependence is stronger that the $t^{1/3}$ dependence noted in Eq. 13, thereby indicating that the curvature of the grain boundary is more important in determining grain growth kinetics than is the surface morphology. Therefore an average grain will increase in size with the second power of distance from the substrate and will not become pinned (at $d \sim \lambda_m$).

IV. MONTE CARLO SIMULATIONS OF ZONE II

Since the mobility of atoms on the surface greatly exceeds that in the bulk, the interior of the film is effectively frozen during deposition (for $T < 0.5\ T_m$). Therefore, all of the microstructural development of the film must occur at the free surface, where the deposition flux is being incorporated into the film. While the surface morphology is determined by the competition between a surface curvature driven instability and surface diffusion, the evolution of the grain size during deposition is determined by grain boundary curvature in the plane of the film. An atom, deposited on the surface of the film, is free to diffuse until the next layer of atoms deposited from the vapor bury it and render it immobile. The area of the surface such an atom samples is dictated by the mean diffusion distance: D_s/J. In diffusing along the surface, the atom samples many different local environments with different atomic site energies. The probability that an atom makes a transition from one site to another in a unit time is

$$P = A e^{\Delta E/K_B T} \tag{15}$$

where ΔE is the difference in energy between the new and old sites, A is a normalization factor, and we have explicitly assumed that the activation energy is identical for all inter-site transitions. While such transitions lead to surface diffusion, they also control the evolution of grain size. Just as the difference in energy between an atom on a flat and curved surface is proportional to the surface energy and curvature, an atom sitting at a grain boundary is sensitive to the grain boundary energy and the curvature of the grain boundary. Therefore an atom at a grain boundary finds it more favorable to join one of the crystals, bounding the grain boundary, than the other, such that the grain boundary migrates towards its center of curvature. Except at early times where the surface curvature may dominate, the evolution of grain size during deposition is determined by the curvature of the grain boundaries intersecting the nominally two dimensional surface.

The method employed in simulating the development of Zone II microstructures is identical to that proposed in Ref. 11, where the interested reader is referred for details. Although this Monte Carlo simulation procedure is essentially two dimensional in nature, the microstructure of real films is three dimensional. The correspondence between the simulation and film relies on the fact that in Zone II the microstructure below the surface is kinetically frozen in and all microstructural evolution occurs at the free surface. Time in the two dimensional simulation corresponds to distance from the substrate (measured normal to the substrate). This relationship is due to the fact that at constant deposition rate, the free surface moves away from the substrate at a fixed velocity. Therefore, the film microstructure (parallel to the surface) at different depths into the film may be obtained from the two dimensional simulated microstructure at different times. Similarly, the microstructure observed on cross-sectioning the film (along any plane containing the substrate normal) is obtained by plotting the position of the grain boundaries at each time step, above the position of the grain boundaries at the previous time step.

The microstructure of a film simulated under conditions of isotropic grain boundary and surface energy are indicated in Figs. 7 and 8. The kinks on the grain boundaries are results of the discreteness of the model and would be invisible in a micrograph of an actual film. Figure 7 shows that the mean grain size increases as the free surface is approached. Most of the grains that were present at the substrate have disappeared by the end of the deposition/growth simulation. Their disappearance is a result of the growth competition between adjacent grains. Some grains are seen (Fig. 7) to initially increase in size, but eventually lose out to the surrounding grains. What appears as nucleation of new grains in Fig. 7 is actually the impingement of a grain which did not initially intersect the plane of the figure. Similarly the apparent coalescence of two grains is attributable to either the advance of a curved grain boundary towards its center of curvature (in a plane parallel to the surface) or the real coalescence of two grains of like orientation. The distribution of grain sizes[12] is found to be independent of the depth of the cross section provided that the grain sizes are normalized by the mean grain size. The grain size distribution is found to be reasonably well fit[12] by:

$$P(A/\langle A \rangle) = e^{-A/\langle A \rangle} \tag{16}$$

where $P(A/\langle A \rangle)$ is the probability that a grain has area $A/\langle A \rangle$. The topological properties of

the microstructure is essentially that observed for normal grain growth in bulk materials.[12] The mean grain size is found[12] to increase with distance from the substrate as $h^{1/2}$, suggesting that the average grain shape in the plane perpendicular to the surface should appear nearly parabolic. Although this predicts an average grain shape, the growth competition makes it impossible to observe such a morphology. The resultant microstructure does however, appear essentially columnar.

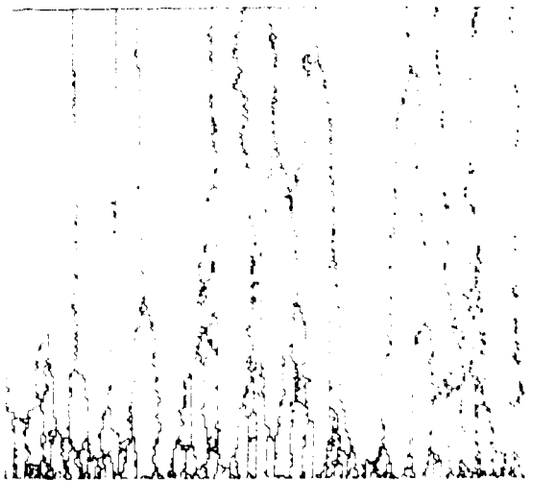

Figure 7. Cross section of the film perpendicular to the surface.

Figure 8. Cross section of the film parallel to the substrate.

Although we have assumed that all surfaces have the same energy, real crystalline materials show surface energy anisotropy. The effect of surface energy anisotropy on grain growth in thin metallic sheets is well known.[13] Providing the sheet is not too thick, surface energy anisotropy can lead to tertiary recrystallization or the fast growth of those grains with low surface energy.[13] One of the hallmarks of this effect is the development of a strong crystallographic texture (i.e the development of preferred crystallographic orientation). Texture effects are also commonly observed in films. In order to study such effects on the microstructural evolution of films, we have introduced a surface energy anisotropy factor into the Hamiltonian of the simulation model (see Eq. 3 of Ref. 11). The initial fraction of grains with low energy orientations, f, is varied in the simulations.

In Figs. 9a-9c, we show simulated microstructures for films grown with f = 0.4, 0.1, and 0.01, respectively. These figures also show the mean grain size, <A>, and the fraction of grains with low surface energy orientations, F, as a function of film thickness. The f = 0.4 film (Fig. 9a) closely resembles the film microstructures observed in the absence of surface energy anisotropy. The transformation to uniformly low energy surface orientation (F = 1) occurs very rapidly and then evolution is controlled solely by grain boundary curvature. The evolution of the mean grain area, for this case, is linear over most of the film thickness, but shows a small perturbation at small heights where the texture is evolving.

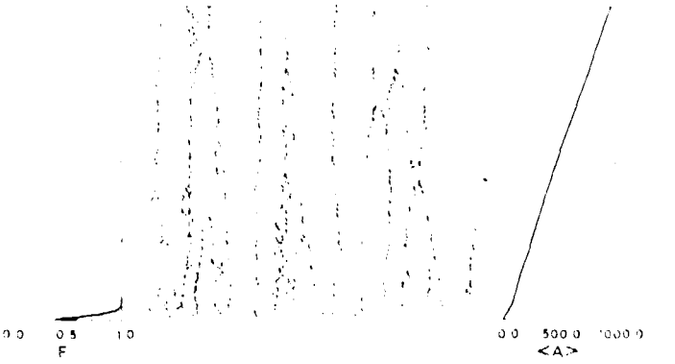

Figure 9a. Cross section of the film perpendicular to the surface, for an initial fraction, f = 0.4, of grains with low energy orientations. Also shown are the mean grain-size <A> and the fraction of grains, F, with low surface energy orientations, as a function of the film thickness.

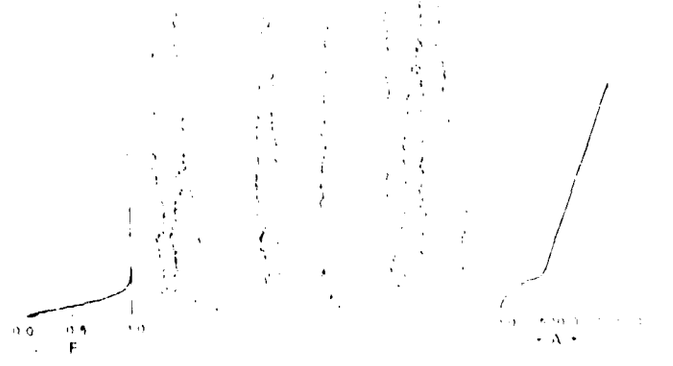

Figure 9b. As in (9a) but for f = 0.1.

These effects become increasingly pronounced with decreasing f (Figs. 9a-9c). The microstructures show a transition from a relatively fine grain size near the substrate to a much more coarse grain size at larger h. This transition occurs at larger h for decreasing f at fixed surface energy anisotropy. The large h grain size also increases with decreasing f. Examination of the F and <A> versus thickness plots show that this transition occurs near F

= 1 (i.e. when the texture development is complete). The parabolic shape of the <A> vs. h plot at small h is due to the initial fast growth of the low surface energy grain into the matrix of high surface energy grains around them. The plots of F versus h (especially for f = 0.01) show a sideways sigmoidal behavior. This behavior may be described in terms of the Johnson-Mehl-Avrami transformation kinetics equation:

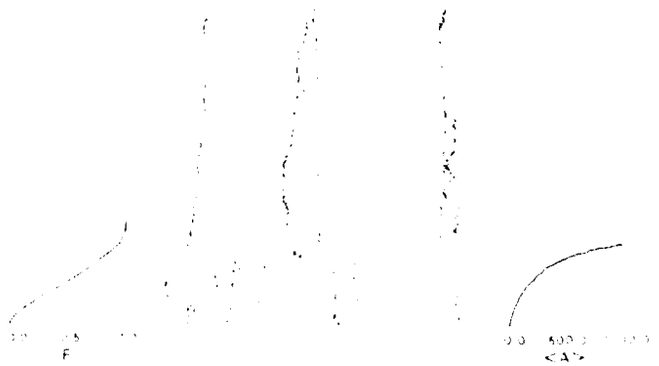

Figure 9c. As in (9a) but for f = 0.01.

$$F = 1 - \exp[-A(h - h_0)^{\alpha}]$$

$$h_0 = \left| (1/A) \ln\left(\frac{1}{1-f}\right) \right|^{1/\alpha} \qquad (17)$$

where A is a constant and α is 2 for the surface energy driven microstructural evolution case. Examination of the microstructure of the film (parallel to the surface) at different depths (Fig. 10) shows a relatively uniform microstructure near the surface and a bimodal grain size distribution at intermediate depths. This variation is due to the non-steady state grain growth occurring while texture evolution is not complete (i.e. F < 1).

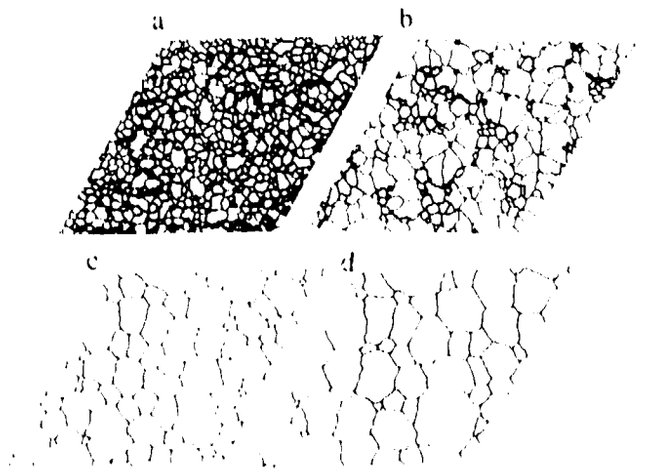

Figure 10. The microstructure of the film (parallel to the substrate) at different depths.

V. CONCLUSION

Theoretical, numerical, and simulation results have been presented which show that columnar, Zone II film microstructures are primarily controlled by the competition between discrete atomic deposition and surface diffusion. This model quantitatively describes the Zone I to Zone II transition temperature, the surface morphology, the columnar grain structure, the film thickness dependence of the grain size, and the development of film texture. Future work will extend the theoretical analysis to two dimensional surfaces, address the effects of atomic shadowing on Zone I microstructures, and elucidate the Zone II to Zone III transition.

REFERENCES

1. B. A. Movchan and A. V. Demchishin, Phys. Met. Metallogr. 28, 83 (1969).
2. J. A. Thornton, Ann. Rev. Mater. Sci. 7, 239 (1977).
3. C. R. M. Grovenor, H. T. G. Hentzell, and D. A. Smith, Acta Metall. 32, 773 (1984); H. T. G. Hentzell, B. Anderson, and S. E. Karlsson, Acta Metall. 31, 2103 (1983).
4. J. A. Thornton, J. Vac. Sci. Technol. 11, 666 (1974).
5. P. Meakin, P. Ramanlal, L. M. Sander, and R. C. Ball, Phys, Rev. A 34, 5091 (1986).
6. B. A. Movchan and A. V. Demchishin, Fizika Metall. 28, 83 (1969).
7. K. H. Müller, J. Appl. Phys. 58, 2573 (1985).
8. D. J. Srolovitz, A. Mazor, P. S. Hagan, and B. G. Bukiet, J. Vac. Sci. Technol., to be published.
9. H. J. Leamy, G. H. Gilmer, and A. G. Dirks, in "Current Topics in Materials Science," ed. E. Kaldis (North-Holland, Amsterdam, 1980), Vol. 6, p. 309.
10. W. W. Mullins, J. Appl. Phys. 28, 333 (1957).
11. D. J. Srolovitz, J. Vac. Sci. Technol. A 4, 2925 (1986).
12. D. J. Srolovitz, M. P. Anderson, G. S. Grest, and P. S. Sahni, Acta Metall. 32, 1429 (1984).
13. C. C. Wong, H. I. Smith, and C. V. Thompson in "Proceedings of the Materials Research Society" (Materials Research Society, Pittsburgh, 1985), Vol. 47, p. 35.